

# Comparison of Standard, Radio-sounded and Forecasted Atmospheric Data in a Solar Spectrum Atmospheric Correction System

L. Martínez, V. Palà, R. Arbiol  
Unitat de Teledetecció  
Institut Cartogràfic de Catalunya (ICC)  
Barcelona, Spain  
lmartinez@icc.es

**Abstract**— A two-step solar spectrum atmospheric correction system is presented in this work. The first step is a semi-empirical model while the second one is empirical. Several atmospheric corrections on a multitemporal series of Landsat 7 panchromatic images have been carried out in order to allow a comparison between standard and operative meteorological atmospheric data. The semi-empirical step consists of a model designed to correct the gaseous absorption and both the atmospheric and aerosol scattering. It includes a radiative transfer simulation module developed from the 6S code that can be used with either standard atmospheric data or meteorological data, such as radio-sounding measurements or MASS forecasted data for each image. The last step is an empirical model based on pseudo-invariant areas found with a Tasseled Cap transformation applied to TOA reflectance on Landsat 7 images. It is designed to compensate for calibration degradation and other factors not taken into account in the first step and requires the use of a multitemporal set of images.

*Solar-spectrum; atmospheric correction; radio-sounding; meteorological forecast; Landsat 7 ETM+.*

## I. INTRODUCTION

Solar-spectrum, passive remote sensing sensors measure mainly the radiance reflected by the atmosphere-ground system, since thermal emissions are insignificant in the solar-spectrum wavelength region. Those images content several kinds of geometric and radiometric distortions. Radiometric distortion should be corrected in order to obtain accurate physical measurements, develop studies based on multitemporal series of images, or compare images acquired with different sensors.

Radiance measured by a sensor depends on illumination geometry and on reflectance characteristics of the observed surface. However, two atmospheric radiative processes disturb this measurement: gas absorption and both Rayleigh and Mie scattering. Absorption is an inelastic energetic process and it is highly wavelength-dependent. On the other hand, scattering is an elastic interaction process with a smooth wavelength dependency that only changes the electromagnetic wave propagation pathway. Rayleigh scattering is caused by gaseous particles, while Mie scattering is due to aerosols. Scattering

causes the adjacent effect: a wrong measurement effect caused by radiation incoming from the surrounding area where the observed surfaced is located. Therefore, each radiance measurement is contaminated in an amount that depends on its neighbouring pixels radiances.

Atmospheric-effect corrected remote sensing measurements are routinely obtained at "Institut Cartogràfic de Catalunya" (ICC) with a self-developed Solar Spectrum Atmospheric Correction System. It consists of a two-step system that links together a semi-empirical method based on a physical model, followed by an empirical method based on normalizing over the time the radiometry of pseudo-invariant areas. The system is modular and it is suitable for any sensor or platform. The semi-empirical step allows the incorporation of synchronous ancillary atmospheric data during the radiative transfer simulation process in order to individually obtain absolute radiance measurements on every image. Later, the empirical step refines the multitemporal series of remote sensed data.

Several meteorological measurements or forecasted data are available from meteorological services like the "Servei Meteorològic de Catalunya" (SMC). Radio-soundings are widely performed, while high precision numerical forecast systems are less frequently performed, but also available. On the other hand, standard atmospheric data will be used if synchronous ancillary data are not available.

## II. ATMOSPHERIC CORRECTION SYSTEM METHODOLOGY

### A. Semi-empirical step

The semi-empirical step is applied to radiance measured by the sensor or Top Of Atmosphere (TOA) radiance; as a result, the corrected reflectance or Bottom Of Atmosphere (BOA) reflectance is obtained.

Equivalent extraterrestrial reflectance or TOA reflectance,  $\rho^*$  can be expressed, in terms of measured radiance  $L^*$  as

$$\rho^* = \frac{\pi \cdot L^*}{\mu_s \cdot E_s} \quad (1)$$

where  $E_s$  is the extraterrestrial solar irradiance and  $\mu_s$  is the zenith solar angle cosine.

Taking into account the interaction phenomena described in [1], it is possible to write the radiance at the sensor, when observing a horizontal surface, as

$$L^* = A \frac{\rho_c}{(1 - \langle \rho_e \rangle S)} + B \frac{\langle \rho_e \rangle}{(1 - \langle \rho_e \rangle S)} + L_a \quad (2)$$

where  $\rho_c$  is the surface corrected reflectance,  $\langle \rho_e \rangle$  is the neighbourhood corrected reflectance,  $S$  is the atmospheric albedo,  $L_a$  is the radiance backscattered to the sensor, and  $A$  and  $B$  are related to the direct and diffuse radiance.

Therefore, the corrected reflectance  $\rho_c$ , or BOA reflectance, for the observed surface is

$$\rho_c = \frac{(L^* - L_a)(1 - \langle \rho_e \rangle S) - \langle \rho_e \rangle B}{A} \quad (3)$$

The parameters  $A$ ,  $B$ ,  $S$  and  $L_a$  characterize both observation and illumination geometries, and the condition of the atmosphere when the image was obtained. Their values depend neither on the observed surface reflectance, nor on the neighbourhood's. Hence, they are calculated from the magnitudes  $L_g$  or radiance entering the sensor from the observed surface, and  $L_p$  or radiance entering the sensor from the neighbourhood of the observed surface and backscattered by the atmosphere towards the sensor. If the surface has a uniform reflectance, those magnitudes will be

$$L_g = A \frac{\rho_c}{1 - S\rho_c} \quad L_p = B \frac{\rho_c}{1 - S\rho_c} + L_a \quad (4)$$

Both  $L_g$  and  $L_p$  can be obtained by means of radiative transfer codes working on direct form. The value of  $A$ ,  $B$ ,  $S$  and  $L_a$  is directly obtained by solving the corresponding equations systems. The radiative transfer simulations are performed using the synchronous atmospheric data available.

The neighbourhood corrected reflectance  $\langle \rho_e \rangle$ , will be obtained using the whole neighbourhood radiometry as if it were a hypothetic single pixel located in a uniform reflectance environment. Its radiometry will be calculated using the neighbourhood's pixels radiometry. Among those hypotheses, the value of the magnitude  $\langle \rho_e \rangle$  will be

$$\langle \rho_e \rangle = \frac{L^* - L_a}{A + B + S(L^* - L_a)} \quad (5)$$

### B. Empirical step

A set of multitemporal images, which have been corrected with the proposed semi-empirical step, is suitable for correction with a pseudo-invariant areas normalization method regardless of illumination or atmospheric conditions throughout the image. This has been one of the drawbacks for a systematic and broad use of these statistical methodologies.

That sort of procedure generates more homogeneous radiometric temporal series compensating for atmospheric characterization deviations, sensor calibration drift, etc [2]. Finally, BOA reflectance for those pseudo-invariant areas is

used to calculate bias and gain coefficients of corrected reflectance along the temporal set.

## III. EXPERIMENTAL RESULTS DISCUSSION

The System has been adapted in order to perform atmospheric correction on a series of six panchromatic images from the sensor Enhanced Thematic Mapper Plus (ETM+) on board of Landsat 7 platform depicted in Table 1. The analysed subscene is located in the Barcelona metropolitan area and is shown in (1). The images set is geometrically oriented in simultaneous adjustment block using the geometric model in [3], and it is geocoded with a nearest neighbour procedure in 15m sized pixels.

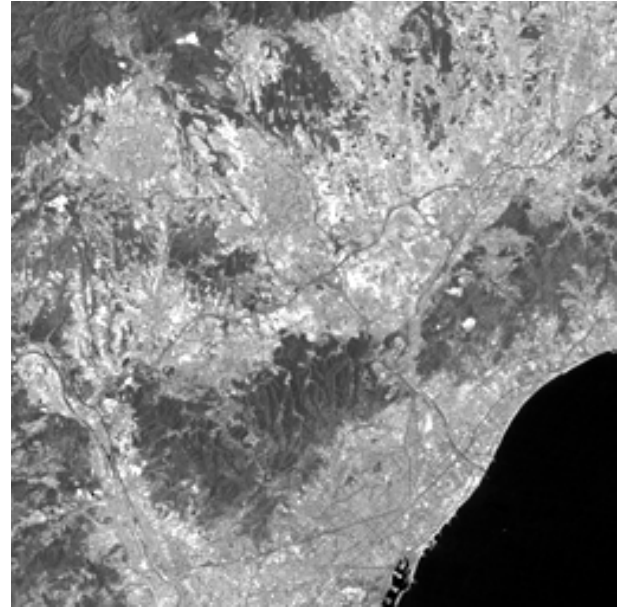


Figure 1. Subscene of Barcelona metropolitan area analysed.

TABLE I. IMAGE SERIES INFORMATION

Acquisition Dates	Acquisition Time (UTC)	Solar Elevation (deg)
23-jul-1999	10:23	60.9°
09-set-1999	10:23	49.2°
30-des-1999	10:23	22.0°
03-mar-2000	10:23	36.7°
07-jun-2000	10:22	64.0°
11-set-2000	10:21	48.1°

Radiative transfer simulation for the application of the physical model has been done using the code Second Simulation of the Satellite Signal in the Solar Spectrum (6S) [4]. The ancillary meteorological data available were:

- World Wide Standard Atmosphere from 6S.
- MASS (Mesoscale Atmospheric Simulation System) [5]. It is a regular tool used at SMC for accurate weather forecasting. On purpose, calculations were performed to obtain data that are almost synchronous (09:00 UTC) with the images capture. Grid spacing

was 15 km and there were values of Temperature, Dew Point, and Geopotential Height, between 1000 and 100 hPa each 25 hPa.

- Radio-sounding profiles are widely used measurements of the physical state of the atmosphere. It is a regular measurement done at SMC twice a day, at 24:00 and 12:00 UTC, from Barcelona. The last one was chosen since it was the closest available to the imagery acquisition.

Besides, a standard climatologic aerosols model, and a Digital Elevation Model of the same resolution as the imagery, was introduced in the simulator system.

Pseudo-invariant areas were chosen by means of a Tasseled Cap transformation (TC) for ETM+ explained in [6]. The total number of pseudo-invariant areas found with that methodology was nine. Those areas had in common low values for the second component of the TC transformation, but with a wide range of values for the first component of the TC transformation. Radiometry values for all those areas were used to perform linear regressions between the images and the first component of the series. Values of  $r^2$  were over 0.98 in all cases. These values show a good pseudo-invariant areas choosing procedure taking into account the shadowing differences over the time present in an urban environment [7].

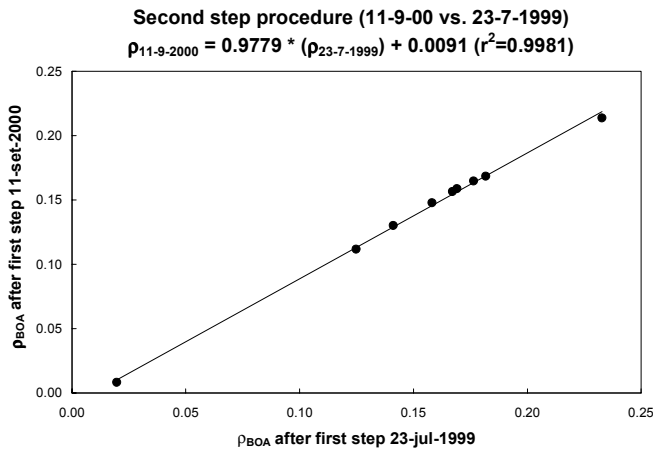


Figure 2. Example of the second step procedure

As it is detailed in Table II, atmospheric uncorrected reflectance or TOA reflectance from the areas established as pseudo-invariant showed a RMS of 0.012 for the whole series. Atmospheric corrected reflectance or BOA reflectance obtained using the semi-empirical method and the Standard Atmosphere had a RMS value of 0.010 for the whole series. Value of the RMS for both the MASS and Radio-sounding data was 0.011. That value is slightly better than the uncorrected one, but does not improve the value resulting when just the Standard Data is used. When the empirical method was applied on data already corrected with the semi-empirical method atmospheric corrected data reduced its RMS value to 0.006, which is half the value before applying the Correction System.

The reduction of RMS obtained with the first step is not very high even incorporating non-standard data, but it must be

noted that this procedure allows the use of the normalization processes regardless of geometric and atmospheric conditions.

TABLE II. RMS OF REFLECTANCE AFTER ATMOSPHERIC CORRECTON

Correction Method Applied	RMS of Reflectance Series
Uncorrected	0.012
Semiempirical step (Standard Data)	0.010
Semiempirical step (MASS Data)	0.011
Semiempirical step (Radio-sounding Data)	0.011
Semiempirical step + Empirical step	0.006

#### IV. CONCLUSIONS

In this work a comparison between standard, radio-sounded and forecasted atmospheric data in a solar spectrum atmospheric correction system has been done. The system has been adapted to perform atmospheric correction on a series of six Landsat 7 ETM+ panchromatic images. Nine pseudo-invariant areas were found by means of a TC transformation.

After performed the correction with a semi-empirical method, the reflectance on pseudo-invariant areas shoed the best RMS using atmospheric standard data, but good results were also obtained when MASS and Radio-sounding data were used. Moreover, this process allowed doing an empirical correction that divided initial RMS value by half, regardless of geometric and atmospheric conditions.

#### ACKNOWLEDGMENTS

The authors are very grateful to Eliseu Vilaclara Ribas and Abdelmalik Sairouni from SMC for MASS forecasted data and atmospheric radio-sounding data delivered. We also are grateful to Fernando Pérez Aragüés from ICC, and all the other reviewers for their helpful suggestions.

#### REFERENCES

- [1] K. Staenz and D.J. Williams, Retrieval of Surface Reflectance from Hiperespectral Data Using a Look-up Table Approach. Canadian Journal of Remote Sensing, Vol 23, n°4, 354-368, 1997.
- [2] V. Caselles and M.J. López, An alternative simple approach to estimate atmospheric correction in multitemporal studies, International Journal of Remote Senging, vol. 10, pp. 1127-1134, 1989.
- [3] V. Palà and X. Pons, Incorporation of relief in polynomial-based geometric corrections, Photogrammetric Engineering and Remote Sensing, vol. 61, pp. 935-944, 1995.
- [4] E. Vermonte, D. Tanré, J.L. Deuzé, M. Herman and J.J. Morcrette, Second simulation of the satellite signal in the solar spectrum, 6S: an overview. IEEE Transactions on Geoscience and Remote Sensing, 35, 675-686, 1997.
- [5] B. Codina, M. Aran, S. Young and A. Redaño, Prediction of a Mesoscale Convective System over Catalonia (Northeastern Spain) with a Nested Numerical Model. Meteor. Atmos. Phys., 62, 9-22, 1997.
- [6] C. Huang, B. Wylie, C. Homer, L. Yang and G. Zylstra, Derivation of a Tasseled cap transformation based on Landsat 7 at-satellite reflectance: International Journal of Remote Sensing, v. 23, no. 8, p. 1741-1748, 2002.
- [7] V. Palà and R. Arbiol, True orthoimage generation in urban areas. Proceedings of 3rd International Symposium Remote Sensing of Urban Areas, vol 1, pp. 309-314. Estambul. 2002.